

Conformal Inference for Online Prediction with Arbitrary Distribution Shifts

Isaac Gibbs* and Emmanuel Candès†

Abstract

Conformal inference is a powerful tool for quantifying the uncertainty around predictions made by black-box models (e.g. neural nets, random forests). Formally, this methodology guarantees that if the training and test data are exchangeable (e.g. i.i.d.) then we can construct a prediction set C for the target Y such that $\mathbb{P}(Y \in C) = 1 - \alpha$ for any target level α . In this article, we extend this methodology to an online prediction setting where the distribution generating the data is allowed to vary over time. To account for the non-exchangeability, we develop a protective layer that lies on top of conformal inference and gradually re-calibrates its predictions to adapt to the observed changes in the environment. Our methods are highly flexible and can be used in combination with any predictive algorithm that produces estimates of the target or its conditional distribution and without any assumptions on the size or type of the distribution shift. We test our techniques on two real-world datasets aimed at predicting stock market volatility and COVID-19 case counts and find that they are robust and adaptive to real-world distribution shifts.

1 Introduction

We consider a situation in which we observe a data stream $\{(X_t, Y_t)\}_{1 \leq t \leq T}$. At each time point t , our goal is to use the previously observed data $\{(X_s, Y_s)\}_{s < t}$, along with the new covariates X_t , to predict the target value Y_t . In many modern applications, this is done using a complex model (e.g. neural network, random forest) that is expensive to train and offers few theoretical guarantees on its test-time performance. There is now a plethora of empirical evidence demonstrating that these models can give highly accurate predictions when given i.i.d. training and testing data. Unfortunately, this provides little assurance in the online prediction setting in which the process generating (X_t, Y_t) may vary over time and successive data points can be correlated. Ideally, this problem can be partially mitigated by only training the predictive model on the most recent data-points. However, with constrained computational resources this can be unrealistic and we may only be able to afford to re-train the model intermittently after many predictions have been made. Thus, the user is often left with few guarantees on the accuracy of the model and little information with which to judge its predictions.

Prediction sets are a useful tool for determining the underlying uncertainty around a model's prediction. Formally, we say that $\hat{C}(\cdot) \subseteq \mathbb{R}$ is a $1 - \alpha$ prediction set for Y if $\mathbb{P}(Y \in \hat{C}(X)) = 1 - \alpha$. The idea is that by examining the size and scope of $\hat{C}(X)$ the user can gain additional information

*Department of Statistics, Stanford University, igibbs@stanford.edu

†Departments of Statistics and Mathematics, Stanford University, candes@stanford.edu

on the utility of a model’s point-prediction of Y . Recently, prediction sets have become quite popular due to the fact that they provide one of the only ways to get a rigorous guarantee on the predictions by machine learning models. This stems from an innovation known as conformal inference, which provides a flexible methodology for transforming point or quantile-estimates into valid prediction sets [see e.g. 21, 6, 18, 10, 17, 5, 1]. Because conformal inference can be used in combination with any underlying predictive model, it can directly leverage improvements in the quality of the initial point or quantile-prediction of the target to obtain small predictions sets [16].

The original conformal inference methods developed by Vovk and colleagues require that all the training and testing data be exchangeable (e.g. be i.i.d.), and in particular require that all points have the same marginal distribution. Recently, many authors have extended this methodology to account for distribution shifts and dependency structures within the training and testing data. Some examples including methods for stationary [4] and non-stationary time series [25], cross-sectional time series [11], label shift [14], covariate shift [20, 24], and general theoretical results on the robustness of classical conformal methods [2].

In this article, we extend the conformal inference framework to settings in which the underlying marginal distribution of (X_t, Y_t) varies smoothly over time. Unlike prior works on this problem [7, 25, 3], we design an algorithm that learns continuously over time and remains fully adaptive to changes in the environment across all time steps. We accomplish this by transforming the coverage problem into an online learning task with a single unknown parameter. We show that our proposed method obtains a coverage rate close to the desired level over any local time interval with an error bound that depends explicitly on the variation of the unknown parameter over time. Thus, in terms of coverage, we simplify the high-dimensional distribution shift in (X_t, Y_t) to a one-dimensional quantity. Finally, we evaluate the performance of our method on two real-world prediction tasks. In the first setting, the goal is to use a sequence of historical stock prices to predict future volatility, while in the second example we use survey data on the community spread of COVID-19 to predict future case counts. We find that in both cases our method produces robust, adaptive prediction sets under real-word dynamics.

2 Methodology

2.1 Conformal inference

Let $(X_1, Y_1), \dots, (X_n, Y_n)$ denote a set of observed training data and (X_{n+1}, Y_{n+1}) denote a new test point from which we only observe X_{n+1} . In order to construct a prediction set for Y_{n+1} , conformal inference inverts a test of $H_0 : Y_{n+1} = y$ for each $y \in \mathbb{R}$. This is accomplished by defining a conformity score $S : (\mathbb{R}^d \times \mathbb{R})^n \times \mathbb{R}^d \times \mathbb{R} \rightarrow \mathbb{R}$ that measures how well the data point (X_{n+1}, y) conforms with $(X_1, Y_1), \dots, (X_n, Y_n)$. We then accept the candidate value y as a plausible value for Y_{n+1} if $S((X_j, Y_j)_{1 \leq j \leq n}, X_{n+1}, y)$ is small relative to $\{S((X_j, Y_j)_{1 \leq j \leq n, j \neq i}, X_{n+1}, y, X_i, Y_i)\}_{1 \leq i \leq n}$. For example, if Y_{n+1} is continuous we could take

$$S((X_j, Y_j)_{1 \leq j \leq n}, X_{n+1}, y) := |y - \hat{\mu}(X_{n+1})|, \quad (2.1)$$

where $\hat{\mu}$ is the result of a regression function fit to $(X_1, Y_1), \dots, (X_n, Y_n), (X_{n+1}, y)$, while if Y_{n+1} is discrete we may set

$$S((X_j, Y_j)_{1 \leq j \leq n}, X_{n+1}, y) := 1 - \hat{\pi}(y | X_{n+1}),$$

where $\hat{\pi}(y|X_{n+1})$ is a fitted estimate of $\mathbb{P}(Y_{n+1} = y|X_{n+1})$. The only requirement on $S(\cdot)$ is that it is unchanged by permutations of its first n arguments. In the context of this article, the data $(X_1, Y_1), \dots, (X_n, Y_n), (X_{n+1}, Y_{n+1})$ will often have a temporal dependence structure. As a result, it may not be sensible to treat all of the arguments to $S(\cdot)$ symmetrically and we will often use conformity scores that are not permutation invariant.

Returning to the original conformal inference setup, let $S_i^y := S((X_j, Y_j)_{1 \leq j \leq n, j \neq i}, X_{n+1}, y, X_i, Y_i)$ and $S_{n+1}^y := S((X_j, Y_j)_{1 \leq j \leq n}, X_{n+1}, y)$. For any $\tau \in \mathbb{R}$ and distribution \mathcal{D} let $\text{Quantile}(\tau, \mathcal{D})$ denote the τ th quantile of \mathcal{D} with the convention that $\text{Quantile}(\tau, \mathcal{D}) = \infty$ (respectively $-\infty$) for all $\tau \geq 1$ (respectively $\tau \leq 1$). Then, conformal inference constructs the prediction set

$$\hat{C}_{n+1} := \left\{ y : S_{n+1}^y \leq \text{Quantile} \left(1 - \alpha, \frac{1}{n+1} \sum_{i=1}^{n+1} \delta_{S_i^y} \right) \right\}. \quad (2.2)$$

As alluded to in the introduction, we have the following rigorous coverage guarantee for \hat{C} .

Theorem 2.1 (Lemma 1 in [16]). *If the data $(X_1, Y_1), \dots, (X_{n+1}, Y_{n+1})$ are exchangeable and $S(\cdot)$ is invariant to permutations of its first n arguments, then*

$$\mathbb{P}(Y_{n+1} \in \hat{C}_{n+1}) \geq 1 - \alpha.$$

Moreover, if in addition all the values $\{S_i^{Y_{n+1}}\}_{1 \leq i \leq n+1}$ are distinct with probability one, then

$$\mathbb{P}(Y_{n+1} \in \hat{C}_{n+1}) \leq 1 - \alpha + \frac{1}{n+1}.$$

The coverage probability upper bound can be strengthened to be exactly $1 - \alpha$ by including a small amount of additional randomization.

Unfortunately, in most practical examples, computing \hat{C}_{n+1} requires us to fit the regression $\hat{\mu}$ for all possible values of y . As this is not usually computationally feasible, many implementations of conformal inference use a data splitting approach in which $\hat{\mu}$ is pre-fit in advance using a separate set of training data [13, 21, 12]. The methods developed in this article do not rely on any formal guarantee of conformal inference and can be used in conjunction with any procedure that produces estimated quantiles of a conformity score. Thus, in our experiments, we avoid extraneous computation by using procedures that do not strictly adhere to the construction given by (2.2).

2.2 Adaptive conformal inference

The methodology developed in this article builds upon the adaptive conformal inference (ACI) algorithm proposed by Gibbs and Candès [7]. This procedure accounts for non-exchangeability by treating the quantile of the conformity scores as a tunable parameter that can be learned in an online fashion. More concretely, let

$$\hat{C}_t(\beta) := \left\{ y : S_t^y \leq \text{Quantile} \left(1 - \beta, \frac{1}{t} \sum_{i=1}^t \delta_{S_i^y} \right) \right\},$$

denote the prediction set obtained using the $1 - \beta$ quantile of the conformity scores. Then, without any assumptions on the data generating distribution, we know that $\beta \mapsto \mathbb{P}(Y_t \in \hat{C}_t(\beta))$ is non-increasing. If, in addition, we make the mild assumption that $\beta \mapsto \mathbb{P}(Y_t \in \hat{C}_t(\beta))$ is continuous,

then there exists an optimal value, α_t^* , such that $\mathbb{P}(Y_t \in \hat{C}_t(\alpha_t^*)) = 1 - \alpha$. Since we do not know this optimal value *a priori*, ACI estimates it in an online fashion using a parameter α_t that is updated as

$$\alpha_t = \alpha_{t-1} + \gamma(\alpha - \text{err}_{t-1}), \quad (2.3)$$

where $\gamma > 0$ is a step-size parameter and

$$\text{err}_{t-1} := \begin{cases} 0, & \text{if } Y_{t-1} \in \hat{C}_{t-1}(\alpha_{t-1}), \\ 1, & \text{if } Y_{t-1} \notin \hat{C}_{t-1}(\alpha_{t-1}). \end{cases}$$

In simple terms, the update (2.3) can be seen as increasing/decreasing the size of the prediction set in response to the historical under/over coverage of the algorithm.

A natural criticism of this approach, originally raised in [3], is that ACI can obtain good coverage not because it successfully learns α_t^* , but rather simply due to the fact that it reactively corrects its past mistakes. In particular, it may be the case that α_t oscillates between being well below and well above α_t^* and thus good coverage is obtained only through a cancellation of positive and negative errors. In Section 4.2 we give empirical evidence indicating that the new methods developed in this article do not show evidence of this pathological behaviour.

The more important difficulty in implementing (2.3) is the choice of γ . Gibbs and Candès [7] give theoretical results suggesting that γ should be chosen proportional to the size of the variation in α_t^* across time. However, this value is unknown and they give no procedure for estimating it. Additionally, much of the theory given in [7] is only valid under two additional assumptions.

1. The conformity score function $S((X_s, Y_s)_{s \leq t}, (X_t, y)) = S(X_t, y)$ is a fixed function that depends only on the new data point (X_t, y) and does not use the most recent data $(X_s, Y_s)_{s \leq t}$ to recalibrate its predictions. For example, under this assumption, the conformity score (2.1) would use a regression function $\hat{\mu}(\cdot)$ that is fixed in advanced and not updated as time progresses.
2. Instead of using the quantiles of the previous conformity scores, $\text{Quantile}(\cdot, \sum_{i=1}^t \frac{1}{t} \delta_{S_i^y})$, we instead have some fixed quantile function, $Q(\cdot)$, that also does not change across time.

These two assumptions are clearly problematic since under distribution shift the most recent data should be used to recalibrate both the predictions made by $\hat{\mu}(\cdot)$ and the estimated distribution of the errors. The most obvious consequence of using fixed models is an increase in the size of the prediction sets over time as the true model drifts and the errors in the point predictions made by $\hat{\mu}(\cdot)$ grow. More subtly, holding $Q(\cdot)$ fixed can cause the coverage probability, $\mathbb{P}(Y_t \in \hat{C}_t)$, to sharply deviate from $1 - \alpha$ as the past conformity scores no longer reflect the current situation. In the following sections, we develop a new method and novel theoretical results that make no assumptions on the way the regression function is fit and thus allow $S(\cdot)$ and $Q(\cdot)$ to be updated over time.

2.3 Fully adaptive conformal Inference

In order to describe our new method, it is useful to first observe that the ACI update (2.3) can be viewed as a gradient descent step with respect to the pinball loss. To see this, let

$$\beta_t := \sup\{\beta : Y_t \in \hat{C}_t(\beta)\},$$

be the value of β such that $\hat{C}_t(\beta_t)$ is the smallest prediction set containing Y_t . Recall the definition of the pinball loss

$$\ell(\beta_t, \theta) := \alpha(\beta_t - \theta) - \min\{0, \beta_t - \theta\}.$$

Then, one can easily verify that (2.3) is equivalent to the update

$$\alpha_t := \alpha_{t-1} - \gamma \nabla_{\theta} \ell(\beta_t, \alpha_t).$$

Through this lens, ACI can be viewed as a gradient descent procedure with respect to the sequence of convex losses $\{\ell(\beta_t, \cdot)\}$. Thus, in order to learn γ we can utilise popular methods from the online convex optimization literature. In particular, we will employ an exponential re-weighting scheme originally proposed by Vovk [22] and refined in [23, 8]. We refer to the resulting procedure as fully adaptive conformal inference (FACI, Algorithm 1). This algorithm takes as input a candidate set of values for γ and constructs a corresponding candidate set of values for α_t by running multiple versions of ACI in parallel. The final value of α_t output at time t is then chosen from these candidate values by evaluating their historical performance. In effect, we learn the optimal value of γ in an online fashion, enabling dynamic calibration of the prediction set to the size of the distribution shift in the environment.

The observant reader may be perplexed to note that Algorithm 1 contains two unknown parameters (namely, σ and η) as opposed to the single unknown value, γ , appearing in the original ACI algorithm. In Section 3, we will outline a simple procedure for choosing σ and η that does not involve any unknown quantities. This contrasts sharply with the situation for γ in which an optimal choice requires an in-depth knowledge of the distribution shift. Additionally, in some environments the size of the distribution shift may vary over time and any single value for γ can be suboptimal. This is not the case for σ and η . Indeed, we will validate empirically that our choices for σ and η lead to good performance in a variety of situations for which any single value of γ fails to provide consistent coverage.

Algorithm 1: FACI, modified version of Algorithm 1 in [8].

Data: Observed values $\{\beta_t\}_{1 \leq t \leq T}$, set of candidate γ values $\{\gamma_i\}_{1 \leq i \leq k}$, starting points $\{\alpha_1^i\}_{1 \leq i \leq k}$, and parameters σ and η .
 $w_1^i \leftarrow 1$, $1 \leq i \leq k$;

for $t = 1, 2, \dots, T$ **do**

Define the probabilities $p_t^i := w_t^i / \sum_{1 \leq j \leq k} w_t^j$, $\forall 1 \leq i \leq k$;
Output $\alpha_t = \alpha_t^i$ with probability p_t^i ;
 $\bar{w}_t^i \leftarrow w_t^i \exp(-\eta \ell(\beta_t, \alpha_t^i))$, $\forall 1 \leq i \leq k$;
 $\bar{W}_t \leftarrow \sum_{1 \leq i \leq k} \bar{w}_t^i$;
 $w_{t+1}^i \leftarrow (1 - \sigma) \bar{w}_t^i + \bar{W}_t \sigma / k$;
 $\text{err}_t^i := \mathbb{1}\{Y_t \notin \hat{C}_t(\alpha_t^i)\}$, $\forall 1 \leq i \leq k$;
 $\text{err}_t := \mathbb{1}\{Y_t \notin \hat{C}_t(\alpha_t)\}$;
 $\alpha_{t+1}^i = \alpha_t + \gamma_i(\alpha - \text{err}_t^i)$, $\forall 1 \leq i \leq k$;

2.4 Additional prior work

Before discussing the theoretical properties of Algorithm 1, we pause to discuss two alternative methods for obtaining adaptive coverage. Most closely related to the present paper is the work of Zaffran et al. [25], which also aims to learn the value of γ in ACI using an aggregation scheme. They investigate a variant of Algorithm 1 in which $\sigma = 0$ and $\eta = \eta_t = O(\sqrt{1/T})$ decays across time and provide empirical evidence that this algorithm produces valid long-term coverage, i.e. for T large, $T^{-1} \sum_{t=1}^T \text{err}_t \cong \alpha$. In Section 3.3, we give a formal proof that with these choices for σ and η , and under no assumptions on the data generating process, or otherwise, $\lim_{T \rightarrow \infty} T^{-1} \sum_{t=1}^T \text{err}_t \stackrel{a.s.}{\equiv} \alpha$.

Unlike [25], we will not use these choices for σ and η . Instead, we advocate for methods that target the correct instantaneous coverage probability across all time steps, i.e. we look to develop methods that achieve $\mathbb{P}(Y_t \notin \hat{C}_t(\alpha_t)) \cong \alpha$, for all t . The choice $\eta_t = O(\sqrt{1/T})$ does not conform to this goal and instead leads to convergence in the learned value for γ , thus depriving the algorithm of adaptivity at larger time-steps. In the original work of Gibbs and Candès [7], the gap between $\mathbb{P}(Y_t \notin \hat{C}_t(\alpha_t))$ and α was shown to explicitly depend on the choice of the step-size. In order to make this gap as small as possible γ needed to be chosen proportional to the size of the distribution shift in the environment. The goal of Algorithm 1 is to adaptively estimate this optimal value for γ and thus obtain the tightest possible bound. On the other hand, the choice $\eta_t = O(\sqrt{1/T})$ can be viewed as implicitly assuming that the size of the distribution shift is constant across time and thus learning only a single value for γ .

The second method we highlight is the multivalid conformal prediction procedure of Bastani et. al. [3]. Instead of targeting the optimal parameter α_t^* , this algorithm chooses α_t in order to explicitly obtain the long-term miscoverage frequency $\lim_{T \rightarrow \infty} T^{-1} \sum_{t=1}^T \text{err}_t = \alpha$. Similar to [25], multivalid conformal also maintains a parameter analogous to η_t , which is sent to 0 as $t \rightarrow \infty$. Thus, this approach also loses adaptivity over time and fails to give any guarantee that $\mathbb{P}(Y_t \notin \hat{C}_t(X)) \cong \alpha$.

3 Coverage properties of FACI

In this section, we outline the main coverage guarantees of FACI. We begin by drawing from known results in the online convex optimization literature that bound a quantity known as the dynamic regret of Algorithm 1. We then draw a connection between this regret and the coverage. Finally, we discuss the long-term coverage in cases where $\eta = \eta_t \rightarrow 0$. All proofs are deferred to the Appendix.

3.1 Dynamic regret of Algorithm 1

Our first result quantifies the error in the expert aggregation scheme by bounding the difference between the loss we obtain and that of the best candidate value.

Lemma 3.1 (Modified version of Lemma 2 in [8]). *Assume that $\sigma \leq 1/2$. Then, for any interval $I = [r, s] \subseteq [T]$ and any $1 \leq i \leq k$,*

$$\sum_{t=r}^s \mathbb{E}[\ell(\beta_t, \alpha_t)] \leq \sum_{t=r}^s \ell(\beta_t, \alpha_t^i) + \eta \sum_{t=r}^s \mathbb{E}[\ell(\beta_t, \alpha_t)^2] + \frac{1}{\eta} (\log(k/\sigma) + |I|2\sigma), \quad (3.1)$$

where the expectation is over the randomness in Algorithm 1 and the data β_1, \dots, β_T can be viewed as fixed.

With this lemma in hand, we now turn to our true target, namely the values α_t^* defined in Section 2.3. Our first step is to recall the following regret bound for gradient descent with a dynamic target.

Lemma 3.2. *For any fixed interval $I = [r, s]$, sequence $\alpha_r^*, \dots, \alpha_s^*$, and $1 \leq i \leq k$,*

$$\sum_{t=r}^s \ell(\beta_t, \alpha_t^i) - \sum_{t=r}^s \ell(\beta_t, \alpha_t^*) \leq \frac{3}{2\gamma_i} (1 + \gamma_i)^2 \left(\sum_{t=r+1}^s |\alpha_t^* - \alpha_{t-1}^*| + 1 \right) + \frac{1}{2} \gamma_i |I|.$$

By combining the previous two lemmas we obtain the main result of this section.

Theorem 3.1. *Let $\gamma_{\max} := \max_{1 \leq i \leq k} \gamma_i$ and assume that $\gamma_1 < \gamma_2 < \dots < \gamma_k$ with $\gamma_{i+1}/\gamma_i \leq 2$ for all $1 < i \leq k$. Assume additionally that $\gamma_k \geq \sqrt{1 + 1/|I|}$ and $\sigma \leq 1/2$. Then, for any interval $I = [r, s] \subseteq [T]$ and any sequence $\alpha_r^*, \dots, \alpha_s^* \in [0, 1]$,*

$$\begin{aligned} \frac{1}{|I|} \sum_{t=r}^s \mathbb{E}[\ell(\beta_t, \alpha_t)] - \frac{1}{|I|} \sum_{r=1}^s \ell(\beta_t, \alpha_t^*) &\leq \frac{\log(k/\sigma) + 2\sigma|I|}{\eta|I|} + \frac{\eta}{|I|} \sum_{t=r}^s \mathbb{E}[\ell(\beta_t, \alpha_t)^2] \\ &\quad + 2\sqrt{3}(1 + \gamma_{\max})^2 \max \left\{ \sqrt{\frac{\sum_{t=r+1}^s |\alpha_t^* - \alpha_{t-1}^*| + 1}{|I|}}, \gamma_1 \right\}, \end{aligned}$$

where the expectation is over the randomness in Algorithm 1 and the data β_1, \dots, β_T can be viewed as fixed.

If we assume that $\gamma_1 \leq \sqrt{\frac{\sum_{t=r+1}^s |\alpha_t^* - \alpha_{t-1}^*| + 1}{|I|}}$ and take the optimal choices $\sigma = 1/(2|I|)$ and $\eta = \sqrt{\frac{\log(k \cdot |I|) + 2}{\sum_{t=r}^s \mathbb{E}[\ell(\beta_t, \alpha_t)^2]}}$, we obtain the much simpler bound,

$$\begin{aligned} \frac{1}{|I|} \sum_{t=r}^s \mathbb{E}[\ell(\beta_t, \alpha_t)] - \frac{1}{|I|} \sum_{r=1}^s \ell(\beta_t, \alpha_t^*) &\leq 2 \sqrt{\frac{\log(k \cdot |I|) + 2}{|I|}} \sqrt{\frac{1}{|I|} \sum_{t=r}^s \ell(\beta_t, \alpha_t)} \\ &\quad + 2\sqrt{3}(1 + \gamma_{\max})^2 \sqrt{\frac{\sum_{t=r+1}^s |\alpha_t^* - \alpha_{t-1}^*| + 1}{|I|}} \\ &= O\left(\sqrt{\frac{\log(|I|)}{|I|}}\right) + O\left(\sqrt{\frac{\sum_{t=r+1}^s |\alpha_t^* - \alpha_{t-1}^*| + 1}{|I|}}\right). \end{aligned}$$

The quantity $\frac{\sum_{t=r+1}^s |\alpha_t^* - \alpha_{t-1}^*|}{|I|}$ can be viewed as a one-dimensional quantification of the size of the distribution shift in the environment. Thus, Theorem A.1 gives a direct control on the average performance of Algorithm 1 in terms of the distribution shift. We emphasize that this result holds over *any* interval $|I|$, justifying our earlier claim that Algorithm 1 is dynamic and adaptive over all time steps.

Unfortunately, the values for σ and η specified above are not usable in practice since they depend on both the size of the time interval $|I|$ and the non-constant value $\sum_{t=r}^s \mathbb{E}[\ell(\beta_t, \alpha_t)]^2$. For this first issue, the user can pick any interval size of interest, with the consideration that choosing

larger intervals gives a tighter bound at the cost of weaker local guarantees. In our experiments, we will set η and σ using the choice $|I| = 500$.

For the second issue, we give two options. The first, is to note that in the idealized setting, where there is no distribution shift, we would have $\beta_t \sim \text{Unif}(0, 1)$ and $\alpha_t^i \cong \alpha_t^* = \alpha$. Plugging in these approximations we obtain

$$\frac{1}{|I|} \sum_{t=r}^s \mathbb{E}[\ell(\beta_t, \alpha_t)^2] \cong \mathbb{E}_{\beta \sim \text{Unif}(0,1)}[\ell(\beta, \alpha)^2] = \frac{(1-\alpha)^2\alpha^3 + \alpha^2(1-\alpha)^3}{3}.$$

Finally, substituting this value into the expression for η above gives the choice $\eta = \sqrt{\frac{3}{|I|}} \sqrt{\frac{\log(k \cdot |I|) + 2}{(1-\alpha)^2\alpha^3 + \alpha^2(1-\alpha)^3}}$.

Our second option, is to simply update η in an online fashion through the equation

$$\eta = \eta_t := \sqrt{\frac{\log(k \cdot 500) + 2}{\sum_{s=t-500}^{t-1} \mathbb{E}[\ell(\beta_s, \alpha_s)^2]}}.$$

This choice would allow us to adaptively track any changes in $\frac{1}{500} \sum_{s=t-500}^{t-1} \mathbb{E}[\ell(\beta_s, \alpha_s)^2]$ across time. In the Appendix, we prove a generalization of Theorem 3.1 that allows $\eta = \eta_t$ to vary across time. We find that a dynamic choice of η_t offers the same regret guarantees as a fixed choice so long as the variability in η_t is not too large. Hence, adaptive values for η_t can be used to minimize the regret bound of Theorem 3.1. On the other hand, empirically, we find that on real data the approximation $\frac{1}{|I|} \sum_{t=r}^s \mathbb{E}[\ell(\beta_t, \alpha_t)^2] \cong \frac{(1-\alpha)^2\alpha^3 + \alpha^2(1-\alpha)^3}{3}$ is highly accurate. Thus, the two different choices for η give nearly identical results in practice. For ease of presentation in the sections that follow we will only display results using the first fixed, heuristic choice of η .

3.2 Bounds on the short-term coverage

The previous section gives bounds on the performance of α_t in terms of the pinball loss $\ell(\beta_t, \alpha_t)$. However, the pinball loss is not our true objective and our real goal is to obtain a value of α_t that is close to α_t^* . Our next result provides a direct connection between bounds on $\ell(\beta_t, \alpha_t)$ and bounds on $(\alpha_t - \alpha_t^*)^2$.

Proposition 3.1. *Let β be a random variable and assume that there exists a value α^* such that $\mathbb{P}(\beta < \alpha^*) = \alpha$. Then, for any τ ,*

$$\mathbb{E}[\ell(\beta, \tau)] - \mathbb{E}[\ell(\beta, \alpha^*)] = \begin{cases} \mathbb{E}[(\tau - \beta) \mathbb{1}_{\alpha^* < \beta \leq \tau}], & \text{if } \tau \geq \alpha^*, \\ \mathbb{E}[(\beta - \tau) \mathbb{1}_{\tau < \beta \leq \alpha^*}], & \text{if } \tau < \alpha^*. \end{cases}$$

So, in particular, if β has a density $p(\cdot)$ on $[0, 1]$ with $p(x) \geq p > 0$ for all $x \in [0, 1]$, then

$$\mathbb{E}[\ell(\tau, \beta)] - \mathbb{E}[\ell(\alpha^*, \beta)] \geq \frac{p(\tau - \alpha^*)^2}{2}.$$

Combining Proposition 3.1 with the results from Section 3.1 we obtain the desired bound on $(\alpha_t - \alpha_t^*)^2$,

$$\frac{1}{|I|} \sum_{t=r}^s \frac{p \mathbb{E}[(\alpha_t - \alpha_t^*)^2]}{2} \leq O\left(\sqrt{\frac{\log(|I|)}{|I|}}\right) + O\left(\sqrt{\frac{\sum_{t=r+1}^s |\alpha_t^* - \alpha_{t-1}^*|}{|I|}}\right), \quad (3.2)$$

where the expectation is now over the randomness in both Algorithm 1 and $\{\beta_s\}_{s < t}$, and p is any lower bound on the density of $\beta_s | \{\beta_r\}_{r < s}, \forall s \leq t$.

In the original work of Gibbs and Candès [7], the authors show that adaptive conformal inference satisfies a nearly identical inequality. However, their result requires three major assumptions: 1) the size of the distribution shift $\frac{\sum_{t=r+1}^s |\alpha_t^* - \alpha_{t-1}^*|}{|I|}$ is known, 2) (X_t, Y_t) is generated by a hidden Markov model, and 3) the regression model is not re-fit across time. In stark contrast, our result makes no such assumptions and, in addition, is adaptive to changes in the size of the distribution shift across time. In practical settings, none of these three assumptions can be reasonably expected to hold and thus our results constitute a significant generalization of those in [7].

3.3 Bounds on the long-term coverage

The results of the previous section show that Algorithm 1 obtains a coverage rate close to $1 - \alpha$ over any local time interval. It is natural to ask if elongating this interval leads to an average coverage of exactly $1 - \alpha$. Here, we show that this is indeed the case if the parameters $\eta = \eta_t \rightarrow 0$ and $\sigma = \sigma_t \rightarrow 0$. This is consistent with other works on online conformal inference that also consider learning rates that decay in time [25, 3], and provides theoretical justification for the empirical results of [25].

Theorem 3.2. *Consider a modified version of Algorithm 1 in which on iteration t the parameters η and σ are replaced by values η_t and σ_t . Let $\gamma_{\min} := \min_i \gamma_i$ and $\gamma_{\max} := \max_i \gamma_i$. Then,*

$$\left| \frac{1}{T} \sum_{t=1}^T \mathbb{E}[\text{err}_t] - \alpha \right| \leq \frac{1 + 2\gamma_{\max}}{T\gamma_{\min}} + \frac{(1 + 2\gamma_{\max})^2}{\gamma_{\min}} \exp(\eta_t(1 + 2\gamma_{\max})) \frac{1}{T} \sum_{t=1}^T \eta_t + 2 \frac{1 + \gamma_{\max}}{\gamma_{\min}} \frac{1}{T} \sum_{t=1}^T \sigma_t,$$

where the expectation is over the randomness in Algorithm 1. So, in particular, if $\lim_{t \rightarrow \infty} \eta_t = \lim_{t \rightarrow \infty} \sigma_t = 0$, then $\lim_{T \rightarrow \infty} \frac{1}{T} \sum_{t=1}^T \text{err}_t \stackrel{a.s.}{=} \alpha$.

As discussed in the previous sections, decaying values of η_t should only be used if the size of the distribution shift in the environment is known to be stationary. Since we do not consider this to be a realistic assumption in most situations, we advocate for using constant or slowly varying values for η . For these choices, we empirically find that Algorithm 1 can produce intervals that are biased in the sense that $\lim_{T \rightarrow \infty} \frac{1}{T} \sum_{t=1}^T \text{err}_t \neq \alpha$. However, in all the examples we have investigated, this bias is sufficiently small to be of little practical consequence.

3.4 Removing randomness in the choice of α_t

In practical settings the randomness in the choice of α_t may be undesirable. To rectify this, we provide an alternative approach that replaces the choice $\alpha_t \sim \sum_{i=1}^k p_t^i \delta_{\alpha_t^i}$ with $\bar{\alpha}_t = \sum_{i=1}^k p_t^i \alpha_t^i$. The full version of this procedure is stated in Algorithm 2. Importantly, this new approach admits the same regret bound as our original procedure.

Corollary 3.1. *Under the same conditions, the conclusion of Theorem 3.1 holds with α_t replaced by $\bar{\alpha}_t$*

Proof. This is an immediate consequence of Jensen's inequality. \square

Unsurprisingly, we find that in practice Algorithms 1 and 2 produce nearly identical results. Thus, we will abuse terminology and also refer to Algorithm 2 as FACI. For simplicity the following sections show results only for Algorithm 2.

Algorithm 2:

Data: Observed values $\{\beta_t\}_{1 \leq t \leq T}$, set of candidate γ values $\{\gamma_i\}_{1 \leq i \leq k}$, starting points $\{\alpha_1^i\}_{1 \leq i \leq k}$, and parameters σ and η .

$w_1^i \leftarrow 1$, $1 \leq i \leq k$;

for $t = 1, 2, \dots, T$ **do**

Define the probabilities $p_t^i := w_t^i / \sum_{1 \leq j \leq k} w_t^j$, $\forall 1 \leq i \leq k$;

Output $\bar{\alpha}_t = \sum_{1 \leq i \leq k} p_t^i \alpha_t^i$;

$\bar{w}_t^i \leftarrow w_t^i \exp(-\eta \ell(\beta_t, \alpha_t^i))$, $\forall 1 \leq i \leq k$;

$\bar{W}_t \leftarrow \sum_{1 \leq i \leq k} \bar{w}_t^i$;

$w_{t+1}^i \leftarrow (1 - \sigma) \bar{w}_t^i + \bar{W}_t \sigma / k$;

$\text{err}_t^i := \mathbb{1}\{Y_t \notin \hat{C}_t(\alpha_t^i)\}$, $\forall 1 \leq i \leq k$;

$\text{err}_t := \mathbb{1}\{Y_t \notin \hat{C}_t(\bar{\alpha}_t)\}$;

$\alpha_{t+1}^i = \alpha_t + \gamma_i(\alpha - \text{err}_t^i)$, $\forall 1 \leq i \leq k$;

4 Real data examples

In this section we investigate the performance of FACI on two real datasets. In all experiments the set of candidate γ values is taken to be $\{0.001, 0.002, 0.004, 0.008, 0.0160, 0.032, 0.064, 0.128\}$. Code for reproducing all of these results can be found at <https://github.com/isgibbs/FACI>.

4.1 Online prediction in the stock market

For our first example, we return to a stock market prediction task that was originally used to evaluate ACI [7]. In this task, the goal is to use the previously observed values of a stock price, $\{P_s\}_{s=0, \dots, t-1}$, to predict its volatility at the next step. The volatility of a stock is defined as the squared value of its return, as given by the equation

$$V_t := \left(\frac{P_t - P_{t-1}}{P_{t-1}} \right)^2.$$

To predict the volatility, we model the stock returns $R_t := \frac{P_t - P_{t-1}}{P_{t-1}}$ as coming from a GARCH(1,1) design. This is a classical financial model for market dynamics in which it is assumed that $R_t = \sigma_t \epsilon_t$ with $\epsilon_t \sim \mathcal{N}(0, 1)$ and

$$\sigma_t^2 = \omega + \tau V_{t-1} + \lambda \sigma_{t-1}^2,$$

for some unknown parameters ω, τ, λ . At each time step, t , we use the most recent 1250 days of returns $\{R_s\}_{t-1250 \leq s < t}$ to produce estimates $\hat{\omega}_t, \hat{\tau}_t, \hat{\lambda}_t$, and $\{\hat{\sigma}_t^s\}_{s < t}$, and a one-step ahead prediction $\hat{\sigma}_t^2 = \hat{\omega}_t + \hat{\tau}_t V_{t-1} + \hat{\lambda}_t (\hat{\sigma}_t^{t-1})^2$. We then construct prediction sets using the equation

$$\hat{C}_t(\alpha_t) := \left\{ v : S_t(v) \leq \text{Quantile} \left(1 - \alpha_t, \frac{1}{1250} \sum_{s=t-1250}^{t-1} \delta_{S_s(V_s)} \right) \right\},$$

where either $S_t(v)$ is taken to be either the normalized conformity score $S_t(v) = |v - (\hat{\sigma}_t^t)^2| / (\hat{\sigma}_t^t)^2$ or the unnormalized score $S_t(v) := |v - (\hat{\sigma}_t^t)^2|$.

In [7] it was found that the normalized and unnormalized conformity scores lead to distribution shifts of drastically different sizes. To see why, observe that if the GARCH(1,1) model is true, and moreover $(\hat{\sigma}_t^2)^2 = \sigma_t^2$ is a highly accurate prediction, then the normalized score satisfies $S_t(V_t) \sim \chi_1^2$, while the unnormalized score follows $S_t(V_t) \sim \sigma_t^2 \chi_1^2$. Thus, if these conditions are met, α_t^* will be invariant across time for the normalized score and highly variable for the unnormalized score. Consistent with this intuition, in [7], it was found that the distribution shift is much larger for the unnormalized score than the normalized score and, thus, in order to obtain good local coverage, ACI requires different (and *a priori* unknown) step sizes for the two scores. On the other hand, as we will show shortly, FACI obtains good performance in both conditions without any prior knowledge of the distribution shift.

In the plots that follow local coverage is measured by the empirical local average coverage rate over a 500-day period defined by

$$\text{LocalCov}_t := 1 - \frac{1}{500} \sum_{t-250+1}^{t+250} \text{err}_t. \quad (4.1)$$

To better understand the behaviour of this quantity, we compute the local coverage rate for both FACI and two baseline methods; a naive baseline, which assumes the data is exchangeable and holds $\alpha_t = \alpha$ fixed, and an optimal baseline, which takes err_t to be an i.i.d. sample from $\text{Bernoulli}(\alpha)$. We call this baseline “optimal” because in the classical case, in which conformal inference is run on a sequence of exchangeable data, $\{\text{err}_t\}$ will be an i.i.d. $\text{Bernoulli}(\alpha)$ sequence [21]. Our goal is to learn the values $\{\alpha_t^*\}$ and recover behaviour similar to the exchangeable case.

Figures 4.1 and 4.2 show the local average coverage rates obtained using the normalized and unnormalized conformity scores on four different stocks. For reference, Figure A.5 in the Appendix shows the prices of the stocks over the same period. All four stocks demonstrate obvious price swings leading to clear distribution shifts in the data. As expected, FACI is able to adapt to both the presence and size of these shifts and obtain a local coverage rate near the target level of $1 - \alpha = 0.9$ over all time steps and conditions. Moreover, we find that the variations in the local coverage rate are similar for both FACI and the i.i.d. Bernoulli sequence indicating that we have recovered performance comparable to the exchangeable case.

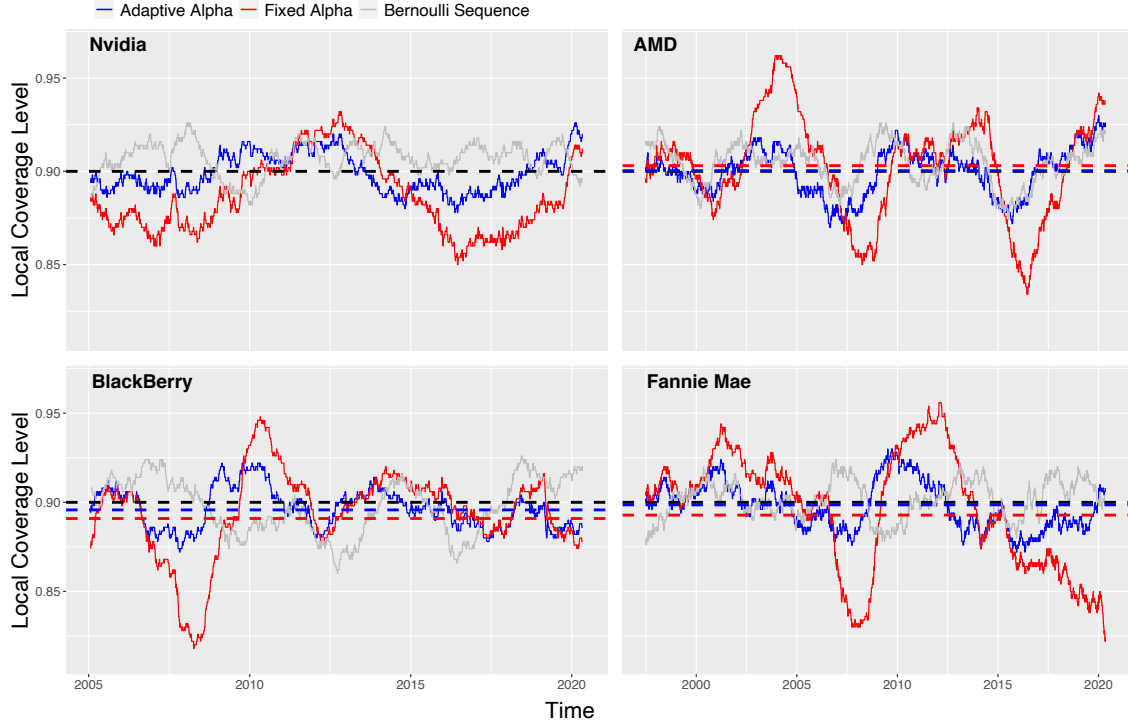


Figure 4.1: Estimation of stock market volatility using conformity score $S_t(v) = |v - (\hat{\sigma}_t^t)^2|/(\hat{\sigma}_t^t)^2$. Solid lines show the local coverage level for $\bar{\alpha}_t$ (blue), a naive baseline that holds $\alpha_t = \alpha$ fixed (red), and an i.i.d. Bernoulli sequence (gray). Dashed lines indicate the global coverage frequency over all time steps for the same methods. The black dashed lines indicates the target level of $1 - \alpha = 0.9$.

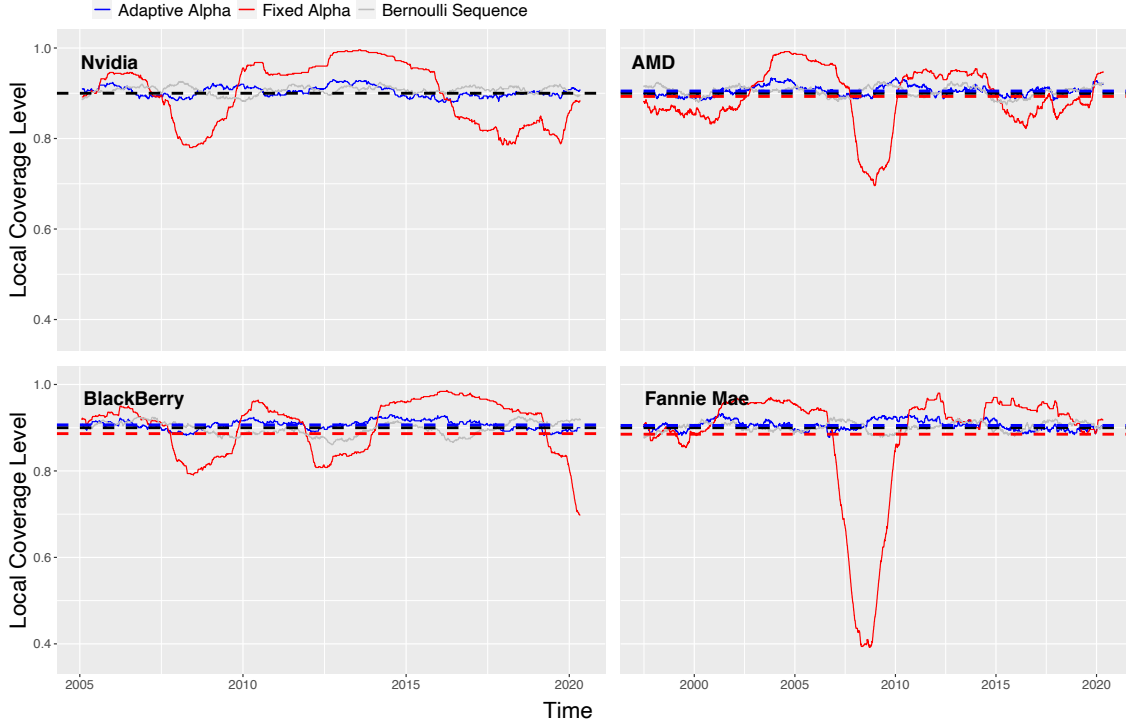


Figure 4.2: Estimation of stock market volatility using conformity score $S_t(v) = |v - (\hat{\sigma}_t^t)^2|$. Solid lines show the local coverage level for $\bar{\alpha}_t$ (blue), a naive baseline that holds $\alpha_t = \alpha$ fixed, (red) and an i.i.d. Bernoulli sequence (gray). Dashed lines indicate the global coverage frequency over all time steps for the same methods. The black dashed lines indicates the target level of $1 - \alpha = 0.9$.

4.2 Evaluating the reactivity of FACI

In [3], adaptive conformal inference was criticized for failing to provide a coverage guarantee conditional on the value of α_t . Indeed, one may be concerned that since ACI acts reactively by widening or shrinking its prediction sets in response to past mistakes, good local coverage is obtained not due to successfully learning α_t^* , but rather as a result of the simple tendency of the algorithm to correct its prior under/over-coverage. Here we gather empirical evidence that demonstrates that FACI is not simply acting reactively.

To do this we divide the interval $[0, 1]$ into m evenly sized sub-intervals B_1, \dots, B_m and evaluate the conditional coverage levels

$$\text{CondCoverage}_i := \frac{1}{|\{t : \bar{\alpha}_t \in B_i\}|} \sum_{t: \bar{\alpha}_t \in B_i} \text{err}_t. \quad (4.2)$$

We apply this to the example in the previous section using the normalized conformity score and display our results in Figure 4.3. As a visual aid, this figure contains error bars indicating the 0.05 and 0.95 quantiles of CondCoverage_i across block bootstrap re-samples of the data (see Algorithm 3 in the Appendix for details). These error bars would give a valid confidence interval for the conditional coverage if, for instance, $\{X_t, Y_t\}$ was a stationary time-series. However, since there is distribution shift in these examples, these error bars are *not* accompanied by any coverage guarantee. Thus, we present them simply as a method to help the reader judge the distance between CondCoverage_i and $1 - \alpha$ relative to the sample size $|\{t : \bar{\alpha}_t \in B_i\}|$.

Overall, we find that almost all of the error bars cover the target level of $1 - \alpha = 0.9$ and for a large majority of the bins, CondCoverage_i is nearly exactly equal to 0.9. If FACI was simply acting reactively to its past mistakes we would expect to observe strong over-coverage at small values of α_t and strong under-coverage at large values of α_t . Thus, Figure 4.3 provides compelling evidence that FACI is not just acting reactively, but rather is successfully learning α_t^* . Similar results were also obtained using the unnormalized conformity scores (see Figure A.4 in the Appendix).

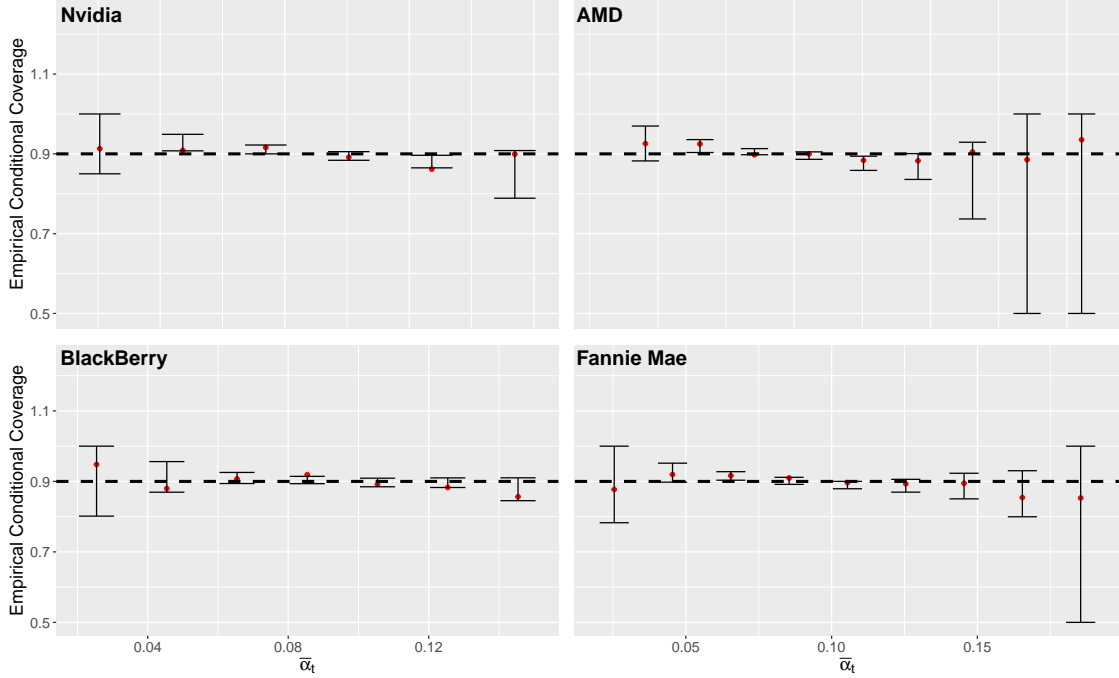


Figure 4.3: Empirical conditional coverage of $\bar{\alpha}_t$ for the estimation of stock market volatility with conformity score $S_t(v) = |v - (\hat{\sigma}_t^t)^2|/(\hat{\sigma}_t^t)^2$. Red points show the empirical conditional coverage given $\bar{\alpha}_t \in B_i$ with error bars indicating the corresponding 0.05 and 0.95 quantiles across 100 block bootstrap resamples of the data $\{(X_i, Y_i)\}$ with block-size set to 100. For visual clarity all error bars are truncated to the range $[0.5, 1]$. Black dashed lines shows the target level of $1 - \alpha = 0.9$.

4.3 Predicting Covid-19 case counts

Over the past two years, researchers have attempted to accurately predict the spread of COVID-19. Here we follow the approach of [19] and consider one simple model for predicting future COVID-19 case counts. In this task, the goal is to make a one-week ahead forecast of the seven day moving average of the number of confirmed cases of COVID-19 in each county in the United States. In order to make these predictions, we utilise Facebook survey data that gives a moving seven day average of the proportion of people who report knowing someone in their local community with COVID-19. All data is obtained from a public repository made available by the DELPHI group at Carnegie Mellon, one of the Center for Disease Control and Prevention's five national centers of excellence for influenza forecasting [15].

Let $\{C_{t,i}\}_{t,i}$ and $\{F_{t,i}\}_{t,i}$ denote the time series of COVID-19 case counts and Facebook survey responses, respectively, where t indexes time and i indexes one of the 3243 counties in the US. At

each time step t we predict $\{C_{t+7,i}\}_i$ by using least-squares regression to fit the model

$$C_{s,i} \sim \beta_0^t + \sum_{j=1}^3 \lambda_j^t C_{s-7j,i} + \sum_{j=1}^3 \kappa_j^t F_{s-7j,i}, \quad s = t - 14, \dots, t, \quad i = 1, \dots, 3243,$$

and setting

$$\hat{C}_{t+7,i} = \hat{\beta}_0^t + \sum_{j=1}^3 \hat{\lambda}_j^t C_{t-7j,i} + \sum_{j=1}^3 \hat{\kappa}_j^t F_{t-7j,i}, \quad i = 1, \dots, 3243.$$

Because survey data is not available for all counties at all time steps, we restrict our analysis to those counties with no missing values in the above expressions.

To compute prediction sets we define the conformity score $S_{t,i} := |\hat{C}_{t,i} - C_{t,i}|/|C_{t-7,i} - C_{t,i}|$ and the count $n_t := |\{i : \text{County } i \text{ has available data at time } t-1\}|$, and set

$$\hat{C}_t(\alpha_{t,i}) := \left\{ c : \frac{|\hat{C}_{t,i} - c|}{|C_{t-7,i} - c|} \leq \text{Quantile} \left(1 - \alpha_t, \frac{1}{n_t} \sum_i \delta_{S_{t-1,i}} \right) \right\}.$$

Since different counties will undergo different dynamics at different stages of the pandemic, we run FACI separately for each county to obtain a set of trajectories $\{\bar{\alpha}_{t,i}\}_i$.

Figure 4.4 shows the empirical local coverage rate over the nearest 200 time steps (i.e equation (4.1), with 250 replaced by 100) for four US counties. These four counties were chosen because they are large urban centres for which data was available over the entire time window we considered. All four of these counties have undergone multiple waves of COVID-19, each of which caused a large swing in the observed case count (see Figure A.6) and thus induced a clear distribution shift into the data. Much like the previous example, we find that FACI successfully corrects for these shifts and maintains a local coverage level near the target at all time steps. This contrasts sharply with the baseline method that holds $\alpha_t = \alpha$ fixed, which, depending on the example, undergoes large swings (e.g. top right panel) or displays a systematic bias (e.g. bottom left panel) away from the target coverage frequency.

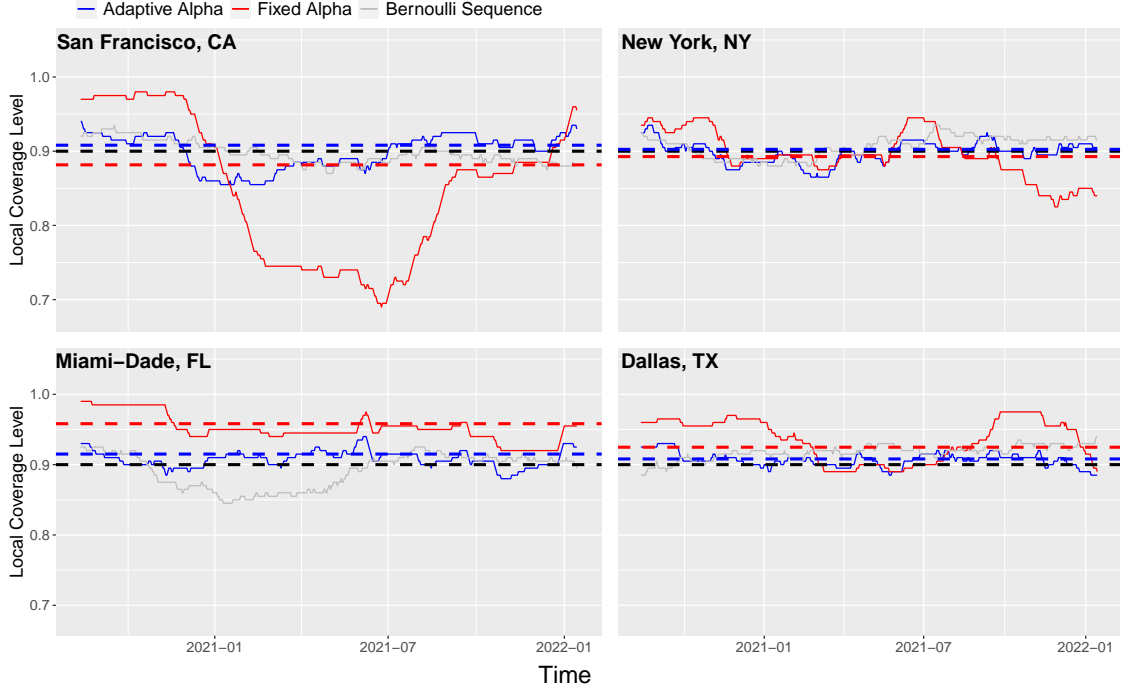


Figure 4.4: Coverage results for the prediction of county-level COVID-19 case counts. Solid lines show the local coverage level for $\bar{\alpha}_t$ (blue), a naive baseline that holds $\alpha_t = \alpha$ fixed (red), and an i.i.d. Bernoulli sequence (gray). Dashed lines indicate the global coverage frequency over all time steps for the same methods. The black dashed lines indicates the target level of $1 - \alpha = 0.9$.

Acknowledgements

E.C. was supported by the Office of Naval Research grant N00014-20-1-2157, the National Science Foundation grant DMS-2032014, the Simons Foundation under award 814641, and the ARO grant 2003514594. I.G. was supported under the Office of Naval Research grant N00014-20-1-2157 and the Simons Foundation under award 814641 as well as by the Overdeck Fellowship Fund. The authors thank Elan Hazan for useful pointers to the online learning literature and John Cherian for helpful comments on an earlier version of this work.

References

- [1] Rina Foygel Barber, Emmanuel J. Candès, Aaditya Ramdas, and Ryan J. Tibshirani. Predictive inference with the jackknife+. *The Annals of Statistics*, 49(1):486 – 507, 2021.
- [2] Rina Foygel Barber, Emmanuel J. Candès, Aaditya Ramdas, and Ryan J. Tibshirani. Conformal prediction beyond exchangeability. *arXiv preprint*, 2022. arXiv:2202.13415.
- [3] Osbert Bastani, Varun Gupta, Christopher Jung, Georgy Noarov, Ramya Ramalingam, and Aaron Roth. Practical adversarial multivalid conformal prediction. *arXiv preprint*, 2022. arXiv:2206.01067.
- [4] Victor Chernozhukov, Kaspar Wüthrich, and Zhu Yinchu. Exact and robust conformal inference methods for predictive machine learning with dependent data. In Sébastien Bubeck, Vianney Perchet, and Philippe Rigollet, editors, *Proceedings of the 31st Conference On Learning Theory*, volume 75 of *Proceedings of Machine Learning Research*, pages 732–749. PMLR, 06–09 Jul 2018.
- [5] Rina Foygel Barber, Emmanuel J Candès, Aaditya Ramdas, and Ryan J Tibshirani. The limits of distribution-free conditional predictive inference. *Information and Inference: A Journal of the IMA*, 08 2020. iaaa017.
- [6] Alexander Gammerman and Vladimir Vovk. Hedging predictions in machine learning. *The Computer Journal*, 50(2):151–163, 2007.
- [7] Isaac Gibbs and Emmanuel Candès. Adaptive conformal inference under distribution shift. In M. Ranzato, A. Beygelzimer, Y. Dauphin, P.S. Liang, and J. Wortman Vaughan, editors, *Advances in Neural Information Processing Systems*, volume 34, pages 1660–1672. Curran Associates, Inc., 2021.
- [8] Paula Gradu, Elad Hazan, and Edgar Minasyan. Adaptive regret for control of time-varying dynamics. *arXiv preprint*, 2020. arXiv:2007.04393.
- [9] Elad Hazan. Introduction to online convex optimization. *arXiv preprint*, 2019. arXiv:1909.05207.
- [10] Jing Lei and Larry Wasserman. Distribution-free prediction bands for non-parametric regression. *Journal of the Royal Statistical Society: Series B (Statistical Methodology)*, 76, 01 2014.
- [11] Zhen Lin, Shubhendu Trivedi, and Jimeng Sun. Conformal prediction with temporal quantile adjustments. *arXiv preprint*, 2022. arXiv:2205.09940.
- [12] Harris Papadopoulos. Inductive conformal prediction: Theory and application to neural networks. In *Tools in Artificial Intelligence*,, pages 315–330, 2008.
- [13] Harris Papadopoulos, Kostas Proedrou, Volodya Vovk, and Alex Gammerman. Inductive confidence machines for regression. In Tapio Elomaa, Heikki Mannila, and Hannu Toivonen, editors, *Machine Learning: ECML 2002*, pages 345–356, Berlin, Heidelberg, 2002. Springer Berlin Heidelberg.

[14] Aleksandr Podkopaev and Aaditya Ramdas. Distribution-free uncertainty quantification for classification under label shift. *arXiv preprint*, 2021. arXiv:2103.03323.

[15] Alex Reinhart, Logan Brooks, Maria Jahja, Aaron Rumack, Jingjing Tang, Sumit Agrawal, Wael Al Saeed, Taylor Arnold, Amartya Basu, Jacob Bien, Ángel A. Cabrera, Andrew Chin, Eu Jing Chua, Brian Clark, Sarah Colquhoun, Nat DeFries, David C. Farrow, Jodi Forlizzi, Jed Grabman, Samuel Gratzl, Alden Green, George Haff, Robin Han, Kate Harwood, Addison J. Hu, Raphael Hyde, Sangwon Hyun, Ananya Joshi, Jimi Kim, Andrew Kuznetsov, Wichada La Motte-Kerr, Yeon Jin Lee, Kenneth Lee, Zachary C. Lipton, Michael X. Liu, Lester Mackey, Kathryn Mazaitis, Daniel J. McDonald, Phillip McGuinness, Balasubramanian Narasimhan, Michael P. O'Brien, Natalia L. Oliveira, Pratik Patil, Adam Perer, Collin A. Politsch, Samyak Rajanala, Dawn Rucker, Chris Scott, Nigam H. Shah, Vishnu Shankar, James Sharpnack, Dmitry Shemetov, Noah Simon, Benjamin Y. Smith, Vishakha Srivastava, Shuyi Tan, Robert Tibshirani, Elena Tuzhilina, Ana Karina Van Nortwick, Valérie Ventura, Larry Wasserman, Benjamin Weaver, Jeremy C. Weiss, Spencer Whitman, Kristin Williams, Roni Rosenfeld, and Ryan J. Tibshirani. An open repository of real-time covid-19 indicators. *Proceedings of the National Academy of Sciences*, 118(51):e2111452118, 2021.

[16] Yaniv Romano, Evan Patterson, and Emmanuel Candès. Conformalized quantile regression. In *Advances in Neural Information Processing Systems*, volume 32. Curran Associates, Inc., 2019.

[17] Mauricio Sadinle, Jing Lei, and Larry Wasserman. Least ambiguous set-valued classifiers with bounded error levels. *Journal of the American Statistical Association*, 114(525):223–234, 2019.

[18] Glenn Shafer and Vladimir Vovk. A tutorial on conformal prediction. *Journal of Machine Learning Research*, 9(12):371–421, 2008.

[19] R. J. Tibshirani. Can symptoms surveys improve covid-19 forecasts? url <https://delphi.cmu.edu/blog/2020/09/21/>. <http://web.archive.org/web/20080207010024/http://www.808multimedia.com/winnt/kernel.htm>, 2020. Accessed: 2022-06-17.

[20] Ryan J Tibshirani, Rina Foygel Barber, Emmanuel Candès, and Aaditya Ramdas. Conformal prediction under covariate shift. In H. Wallach, H. Larochelle, A. Beygelzimer, F. d'Alché-Buc, E. Fox, and R. Garnett, editors, *Advances in Neural Information Processing Systems*, volume 32. Curran Associates, Inc., 2019.

[21] Vladimir Vovk, Alex Gammerman, and Glenn Shafer. *Algorithmic Learning in a Random World*. Springer-Verlag, Berlin, Heidelberg, 2005.

[22] Volodimir G. Vovk. Aggregating strategies. In *Proceedings of the Third Annual Workshop on Computational Learning Theory*, COLT '90, page 371–386, San Francisco, CA, USA, 1990. Morgan Kaufmann Publishers Inc.

[23] Olivier Wintenberger. Optimal learning with bernstein online aggregation. *Mach. Learn.*, 106(1):119–141, jan 2017.

[24] Yachong Yang, Arun Kumar Kuchibhotla, and Eric Tchetgen Tchetgen. Doubly robust calibration of prediction sets under covariate shift. *arXiv preprint*, 2022. arXiv:2203.01761.

[25] Margaux Zaffran, Aymeric Dieuleveut, Olivier Féron, Yannig Goude, and Julie Josse. Adaptive conformal predictions for time series. *arXiv preprint*, 2020. arXiv:2202.07282.

A Appendix

A.1 Details of the block bootstrap for Section 4.2

Algorithm 3 below outlines the block bootstrap procedure used to generate the error bars in Figures 4.3 and A.4. Both figures were generated using the choices $M = 100$ and $b = 100$.

Algorithm 3: Block bootstrap

Data: Sequence of stock returns $\{R_t\}_{1 \leq t \leq T}$, number of bootstrap samples M , block size b , partition B_1, \dots, B_k of $[0, 1]$.

Define the blocks of data $D_i := \{R_{ib+1}, \dots, R_{(i+1)b}\}$, $0 \leq i \leq T/b - 1$;

for $j = 1, 2, \dots, M$ **do**

 Sample $i_1^j, \dots, i_{T/b-1}^j \stackrel{\text{i.i.d.}}{\sim} \text{Unif}(\{0, \dots, T/b - 1\})$;

 Run the procedure outlined in Section 4.1 on dataset $\{D_{i_1^j}, \dots, D_{i_{T/b-1}^j}\}$ to obtain

 sequences $\{\bar{\alpha}_t^j\}_{1 \leq t \leq T}$ and $\{\text{err}_t^j\}_{1 \leq t \leq T}$;

 For $1 \leq \ell \leq k$ compute

$$\text{CondCoverage}_\ell^j := \frac{1}{|\{t : \bar{\alpha}_t^j \in B_\ell\}|} \sum_{t: \bar{\alpha}_t^j \in B_\ell} \text{err}_t^j.$$

For all $1 \leq \ell \leq k$ output the 0.05 and 0.95 empirical quantiles of $\{\text{CondCoverage}_\ell^j\}_{1 \leq j \leq M}$.

A.2 Proofs for Section 3.1

This section contains the proofs of Lemmas 3.1 and 3.2 as well as of Theorem 3.1. In addition we prove a modified version of Theorem 3.1 that allows η to vary over time. We begin by proving the results stated in Section 3.1.

Proof of Lemma 3.1. We follow the calculations of [8]. Let $\ell(\beta_t) := (\ell(\beta_t, \alpha_t^1), \dots, \ell(\beta_t, \alpha_t^k))$, $\ell(\beta_t)^2 := (\ell(\beta_t, \alpha_t^1)^2, \dots, \ell(\beta_t, \alpha_t^k)^2)$ and $p_t := (p_t^1, \dots, p_t^k)$. By construction notice that $W_t = \bar{W}_t$. Thus, using the inequalities $\exp(-x) \leq 1 - x + x^2 \leq \exp(-x + x^2)$ we find that

$$\frac{W_{t+1}}{W_t} = \sum_{i=1}^k p_t^i \exp(-\eta \ell(\beta_t, \alpha_t^i)) \leq \exp(-\eta p_t^T \ell(\beta_t) + \eta^2 p_t^T \ell(\beta_t)^2),$$

and thus inductively

$$\frac{W_{s+1}}{W_r} \leq \exp \left(- \sum_{t=r}^s \eta p_t^T \ell(\beta_t) + \eta^2 p_t^T \ell(\beta_t)^2 \right).$$

On the other hand, for any i , $w_{t+1}^i \geq w_t^i (1 - \sigma) \exp(-\eta \ell(\beta_t, \alpha_t^i))$ which gives

$$\frac{W_{s+1}}{W_r} \geq \frac{w_{s+1}^i}{W_r} \geq (1 - \sigma)^{|I|} \exp \left(- \sum_{t=r}^s \eta \ell(\beta_t, \alpha_t^i) \right) p_r^i \geq (1 - \sigma)^{|I|} \exp \left(- \sum_{t=r}^s \eta \ell(\beta_t, \alpha_t^i) \right) \frac{\sigma}{k}.$$

Combining these two inequalities and taking a logarithm yields

$$\log(\sigma/k) + |I| \log(1 - \sigma) - \sum_{t=r}^s \eta \ell(\beta_t, \alpha_t^i) \leq - \sum_{t=1}^s \eta p_t^T \ell(\beta_t) + \eta^2 p_t^T \ell(\beta_t)^2.$$

Finally, since $\sigma \leq 1/2$ we may use the inequality $\log(1 - \sigma) \geq -2\sigma$ to get the final result

$$\sum_{t=r}^s \mathbb{E}[\ell(\beta_t, \alpha_t)] \leq \sum_{t=r}^s \ell(\beta_t, \alpha_t^i) + \eta \sum_{t=r}^s \ell(\beta_t, \alpha_t)^2 + \frac{1}{\eta} (\log(k/\sigma) + |I|2\sigma).$$

□

Proof of Lemma 3.2. Lemma 4.1 in [7] shows that for all values t , $\alpha_t^i \in [-\gamma_i, 1 + \gamma_i]$. Since $\beta_t \in [0, 1]$ we then also have that $\ell_t(\beta_t, \alpha_t^i) \leq \max\{\alpha, 1 - \alpha\}|\beta_t - \alpha_t^i| \leq 1 + \gamma_t$. Plugging this fact into Theorem 10.1 of [9] gives the result. □

Proof of Theorem 3.1. Fix any $i \in [k]$ and write

$$\sum_{t=r}^s \mathbb{E}[\ell(\beta_t, \alpha_t)] - \sum_{t=r}^s \ell(\beta_t, \alpha_t^*) = \left(\sum_{t=r}^s \mathbb{E}[\ell(\beta_t, \alpha_t)] - \sum_{t=r}^s \ell(\beta_t, \alpha_t^i) \right) + \left(\sum_{t=r}^s \ell(\beta_t, \alpha_t^i) - \sum_{t=r}^s \ell(\beta_t, \alpha_t^*) \right).$$

Applying Lemma 3.1 to the first term and Lemma 3.2 to the second term gives

$$\begin{aligned} \sum_{t=r}^s \mathbb{E}[\ell(\beta_t, \alpha_t)] - \sum_{t=r}^s \ell(\beta_t, \alpha_t^*) &\leq \eta \sum_{t=r}^s \mathbb{E}[\ell(\beta_t, \alpha_t)^2] + \frac{1}{\eta} (\log(|E|/\sigma) + |I|2\sigma) \\ &\quad + \frac{3}{2\gamma_i} (1 + \gamma_i)^2 \left(\sum_{t=r+1}^s |\alpha_t^* - \alpha_{t-1}^*| + 1 \right) + \frac{1}{2} \gamma_i |I|. \end{aligned}$$

Now, there are two cases. If

$$\sqrt{\frac{\sum_{t=r+1}^s |\alpha_t^* - \alpha_{t-1}^*| + 1}{|I|}} \geq \gamma_i \tag{A.1}$$

then since $\sqrt{\frac{\sum_{t=r+1}^s |\alpha_t^* - \alpha_{t-1}^*| + 1}{|I|}} \leq \sqrt{1 + 1/|I|} \leq \gamma_k$ we may find a value γ_i such that

$$\sqrt{\frac{\sum_{t=r+1}^s |\alpha_t^* - \alpha_{t-1}^*| + 1}{|I|}} \leq \gamma_i \leq 2 \sqrt{\frac{\sum_{t=r+1}^s |\alpha_t^* - \alpha_{t-1}^*| + 1}{|I|}}.$$

Plugging this value into the previous expression gives the desired result. Otherwise if (A.1) does not hold, then we may simply plug in γ_1 for γ_i . □

We conclude this section by stating and proving a modified version of Theorem 3.1 that allows η to vary over time. In particular, we consider a modified version of Algorithm 1 in which the update for \bar{w}_t^i is replaced by $\bar{w}_t^i \leftarrow w_t^i \exp(-\eta_t \ell_t(\alpha_t^i))$. We find that if the variation in η_t is of order $1/\sqrt{L}$, FACI will have dynamic regret of size $O(\sqrt{\log(L)/L} + \max\{\gamma_1, \frac{1}{L} \sum_{t=r+1}^s |\alpha_t^* - \alpha_{t-1}^*|\})$.

The primary case of interest is that in which $\eta_t = \sqrt{\frac{\log(L \cdot k) + 2}{\sum_{s=t-L}^{t-1} \mathbb{E}[\ell(\beta_s, \alpha_s)^2]}}$ and $\sigma_t = \frac{1}{2L}$ for some fixed interval length L . Here the assumption that η_t has small variability is motivated by the original work of Gibbs and Candès [7]. In that article the data (X_t, Y_t) are assumed to come from a hidden Markov model and $\hat{C}_t(\cdot)$ is only allowed to depend on a fixed number of previous data points, i.e. $\hat{C}_t(\cdot)$ is computed using only $\{(X_s, Y_s)\}_{t-b \leq s \leq t} \cup \{X_t\}$ for some fixed value b . This is motivated by the idea that in a dynamic environment only the most recent data should be used to compute the conformity scores. In this case $(\beta_t, (\alpha_t^i, p_t^i)_{i \in [k]})$ forms a Markov chain and thus it is reasonable to expect $\sum_{s=t-L}^{t-1} \mathbb{E}[\ell(\beta_s, \alpha_s)^2]$ to have variations of order \sqrt{L} .

Theorem A.1. *Let $L \in \mathbb{N}$ denote a fixed target interval length and $I = [r, s]$ be any interval of length L with $r > L$. For all $t > L$ set $\eta_t := \sqrt{\frac{\log(L \cdot k) + 2}{\sum_{s=t-L}^{t-1} \mathbb{E}[\ell(\beta_s, \alpha_s)^2]}}$ and $\sigma = 1/(2L)$. Assume that*

$$\frac{1}{L\eta_s} \sum_{t=r}^s |\eta_t - \eta_s|, \frac{1}{L\eta_s} \sum_{t=r}^s |\eta_t^2 - \eta_s^2| \leq O\left(\frac{1}{\sqrt{L}}\right)$$

Then, under the conditions of Theorem 3.1

$$\begin{aligned} \frac{1}{L} \sum_{t=r}^s \mathbb{E}[\ell(\beta_t, \alpha_t)] - \frac{1}{L} \sum_{r=1}^s \ell(\beta_t, \alpha_t^*) &\leq 2\sqrt{\frac{\log(2kL) + 2}{L}} \sqrt{\frac{1}{L} \sum_{t=r}^s \mathbb{E}[\ell(\beta_t, \alpha_t)^2]} \\ &\quad + 2\sqrt{3}(1 + \gamma_{\max})^2 \max \left\{ \sqrt{\frac{\sum_{t=r+1}^s |\alpha_t^* - \alpha_{t-1}^*| + 1}{L}}, \gamma_1 \right\} \\ &\quad + O\left(\frac{1}{\sqrt{L}}\right) \\ &= O\left(\sqrt{\frac{\log(L)}{L}}\right) + O\left(\max\{\gamma_1, \frac{1}{L} \sum_{t=r+1}^s |\alpha_t^* - \alpha_{t-1}^*|\}\right), \end{aligned}$$

where the expectation is over the randomness in Algorithm 1. The data β_1, \dots, β_T can be viewed as fixed.

Proof. Proceeding identically the the proof of Lemma 3.1 we have that for any $i \in [k]$

$$\sum_{t=r}^s \eta_t \mathbb{E}[\ell(\beta_t, \alpha_t)] \leq \sum_{t=r}^s \eta_t \ell(\beta_t, \alpha_t^i) + \sum_{t=r}^s \eta_t^2 \mathbb{E}[\ell(\beta_t, \alpha_t)^2] + \log(k/\sigma) + |I|2\sigma$$

Now, by Lemma 4.1 of [7] we know that $\alpha_t^i \in [-\gamma_i, 1 + \gamma_i]$ and thus that $\ell(\beta_t, \alpha_t) \leq 1 + \gamma_{\max}$. Hence,

$$\eta_s \sum_{t=r}^s \mathbb{E}[\ell(\beta_t, \alpha_t)] \leq \eta_s \sum_{t=r}^s \ell(\beta_t, \alpha_t^i) + \eta_s^2 \sum_{t=r}^s \mathbb{E}[\ell(\beta_t, \alpha_t)^2] + \log(k/\sigma) + |I|2\sigma + \sum_{t=r}^s |\eta_t - \eta_s| + \sum_{t=r}^s |\eta_t^2 - \eta_s^2|.$$

The proof remainder of the proof is identical to that of Theorem 3.1. □

A.3 Proofs for Section 3.2

In this section we prove Proposition 3.1.

Proof. For simplicity we will only prove the case where $\tau > \alpha^*$. The case where $\tau \leq \alpha^*$ is identical. By a direct computation we have that

$$\begin{aligned}
& \mathbb{E}[\ell(\tau, \beta)] - \mathbb{E}[\ell(\alpha^*, \beta)] \\
&= \mathbb{E}[\alpha(\beta - \tau) \mathbb{1}_{\beta \geq \tau}] + \mathbb{E}[(1 - \alpha)(\alpha^* + \epsilon - \beta) \mathbb{1}_{\beta < \tau}] - \mathbb{E}[\alpha(\beta - \alpha^*) \mathbb{1}_{\beta \geq \alpha^*}] \\
&\quad - \mathbb{E}[(1 - \alpha)(\alpha^* - \beta) \mathbb{1}_{\beta < \alpha^*}] \\
&= -\mathbb{E}[\alpha(\tau - \alpha^*) \mathbb{1}_{\beta \geq \tau}] + \mathbb{E}[(1 - \alpha)(\tau - \alpha^*) \mathbb{1}_{\beta < \alpha^*}] + \mathbb{E}[(1 - \alpha)(\tau - \beta) - \alpha(\beta - \alpha^*)] \mathbb{1}_{\alpha^* \leq \beta < \tau} \\
&= -\mathbb{E}[\alpha(\tau - \alpha^*) \mathbb{1}_{\beta \geq \alpha^*}] + \mathbb{E}[(1 - \alpha)(\tau - \alpha^*) \mathbb{1}_{\beta < \alpha^*}] + \mathbb{E}[\alpha(\tau - \alpha^*) \mathbb{1}_{\alpha^* \leq \beta < \tau}] \\
&\quad + \mathbb{E}[(1 - \alpha)(\tau - \alpha^*) \mathbb{1}_{\alpha^* \leq \beta < \tau}] - \mathbb{E}[(\beta - \alpha^*) \mathbb{1}_{\alpha^* \leq \beta < \tau}] \\
&= -\alpha(1 - \alpha)(\tau - \alpha^*) + \alpha(1 - \alpha)(\tau - \alpha^*) + \mathbb{E}[(\tau - \alpha^*) \mathbb{1}_{\alpha^* \leq \beta < \tau}] - \mathbb{E}[(\beta - \alpha^*) \mathbb{1}_{\alpha^* \leq \beta < \tau}] \\
&= \mathbb{E}[(\tau - \beta) \mathbb{1}_{\alpha^* \leq \beta < \tau}].
\end{aligned}$$

This proves the first part of Proposition 3.1. For the second part note that if β has a density on $[0, 1]$ that is lower bounded by p , then

$$\mathbb{E}[(\tau - \beta) \mathbb{1}_{\alpha^* \leq \beta < \tau}], \mathbb{E}[(\beta - \tau) \mathbb{1}_{\tau \leq \beta < \alpha^*}] \geq \int_0^{\tau - \alpha^*} x p dx = p \frac{(\tau - \alpha^*)^2}{2}.$$

□

A.4 Proofs for Section 3.2

In this section we prove Theorem 3.2.

Proof Of Theorem 3.2. Let

$$\tilde{\alpha}_t := \sum_i \frac{p_t^i \alpha_t^i}{\gamma_i}$$

and observe that

$$\begin{aligned}
\tilde{\alpha}_t &= \sum_i \frac{p_t^i (\alpha_{t+1}^i - \gamma_i(\alpha - \text{err}_t^i))}{\gamma_i} = \sum_i \frac{p_t^i \alpha_{t+1}^i}{\gamma_i} + \sum_i p_t^i (\text{err}_t^i - \alpha) \\
&= \tilde{\alpha}_{t+1} + \sum_i \frac{(p_t^i - p_{t+1}^i) \alpha_{t+1}^i}{\gamma_i} + \sum_i p_t^i (\text{err}_t^i - \alpha).
\end{aligned}$$

Thus,

$$\mathbb{E}[\text{err}_t] - \alpha = \tilde{\alpha}_t - \tilde{\alpha}_{t+1} + \sum_i \frac{(p_{t+1}^i - p_t^i) \alpha_{t+1}^i}{\gamma_i}. \quad (\text{A.2})$$

Now, for ease of notation let $W_t := \sum_i w_t^i$ and $\tilde{p}_{t+1}^i := \frac{p_t^i \exp(-\eta_t \ell(\beta_t, \alpha_t^i))}{\sum_{i'} p_t^{i'} \exp(-\eta_t \ell(\beta_t, \alpha_t^{i'}))}$. Recall that by definition,

$$p_{t+1}^i = \frac{w_{t+1}^i / W_t}{\sum_{i'} w_{t+1}^{i'} / W_t} = (1 - \sigma_t) \tilde{p}_{t+1}^i + \frac{\sigma_t}{k}.$$

Now, by a direct computation

$$\begin{aligned}
\tilde{p}_{t+1}^i - p_t^i &= \frac{p_t^i \exp(-\eta_t \ell(\beta_t, \alpha_t^i))}{\sum_{i'} p_t^{i'} \exp(-\eta_t \ell(\beta_t, \alpha_t^{i'}))} - p_t^i \\
&= p_t^i \frac{\exp(-\eta_t \ell(\beta_t, \alpha_t^i)) - \sum_{i'} p_t^{i'} \exp(-\eta_t \ell(\beta_t, \alpha_t^{i'}))}{\sum_{i'} p_t^{i'} \exp(-\eta_t \ell(\beta_t, \alpha_t^{i'}))} \\
&= p_t^i \frac{\sum_{i'} p_t^{i'} (\exp(-\eta_t \ell(\beta_t, \alpha_t^i)) - \exp(-\eta_t \ell(\beta_t, \alpha_t^{i'})))}{\sum_{i'} p_t^{i'} \exp(-\eta_t \ell(\beta_t, \alpha_t^{i'}))} \\
&= p_t^i \frac{\sum_{i'} p_t^{i'} \exp(-\eta_t \ell(\beta_t, \alpha_t^{i'})) (\exp(\eta_t \ell(\beta_t, \alpha_t^{i'})) - \eta_t \ell(\beta_t, \alpha_t^i)) - 1}{\sum_{i'} p_t^{i'} \exp(-\eta_t \ell(\beta_t, \alpha_t^{i'}))} \\
&= p_t^i \sum_{i'} \tilde{p}_{t+1}^{i'} (\exp(\eta_t \ell(\beta_t, \alpha_t^{i'})) - \eta_t \ell(\beta_t, \alpha_t^i)) - 1.
\end{aligned}$$

By Lemma 4.1 of [7] we know that $\alpha_t^i \in [-\gamma_i, 1 + \gamma_i]$ and thus that $|\ell(\beta_t, \alpha_t^{i'}) - \ell(\beta_t, \alpha_t^i)| \leq \max\{\alpha, 1 - \alpha\}|\alpha_t^{i'} - \alpha_t^i| \leq 1 + 2\gamma_{\max}$. Hence, by the intermediate value theorem

$$|\exp(\eta_t \ell(\beta_t, \alpha_t^{i'})) - \exp(\eta_t \ell(\beta_t, \alpha_t^i)) - 1| \leq \eta_t (1 + 2\gamma_{\max}) \exp(\eta_t (1 + 2\gamma_{\max})),$$

and thus also

$$|\tilde{p}_{t+1}^i - p_t^i| \leq p_t^i \eta_t (1 + 2\gamma_{\max}) \exp(\eta_t (1 + 2\gamma_{\max})).$$

Applying Lemma 4.1 of [7] again we conclude that

$$\begin{aligned}
\left| \sum_i \frac{(\tilde{p}_{t+1}^i - p_t^i) \alpha_{t+1}^i}{\gamma_i} \right| &\leq (1 - \sigma_t) \sum_i \left| \frac{(\tilde{p}_{t+1}^i - p_t^i) \alpha_{t+1}^i}{\gamma_i} \right| + \sigma_t \sum_i \left| \frac{(p_{t+1}^i - p_t^i) \alpha_{t+1}^i}{\gamma_i} \right| \\
&\leq \frac{\eta_t (1 + 2\gamma_{\max})^2}{\gamma_{\min}} \exp(\eta_t (1 + 2\gamma_{\max})) + 2\sigma \frac{1 + \gamma_{\max}}{\gamma_{\min}}.
\end{aligned}$$

So, taking a sum over t in equation A.2 gives the inequality

$$\left| \frac{1}{T} \sum_t \mathbb{E}[\text{err}_t] - \alpha \right| \leq \frac{|\tilde{\alpha}_1 - \tilde{\alpha}_{T+1}|}{T} + \frac{(1 + 2\gamma_{\max})^2}{\gamma_{\min}} \exp(\eta_t (1 + 2\gamma_{\max})) \frac{1}{T} \sum_{t=1}^T \eta_t + 2 \frac{1 + \gamma_{\max}}{\gamma_{\min}} \frac{1}{T} \sum_{t=1}^T \sigma_t.$$

Applying Lemma 4.1 of [7] one final time gives $\gamma_{\min} \tilde{\alpha}_t \in [-\gamma_{\max}, 1 + \gamma_{\max}]$ and thus $|\tilde{\alpha}_1 - \tilde{\alpha}_{T+1}| \leq (1 + 2\gamma_{\max})/\gamma_{\min}$. Plugging this into the previous expression gives the desired upperbound.

Finally, if $\eta_t, \sigma_t \rightarrow 0$ then applying the law of large numbers gives

$$\lim_{T \rightarrow \infty} \left| \frac{1}{T} \sum_t \text{err}_t - \alpha \right| = \lim_{T \rightarrow \infty} \left| \frac{1}{T} \sum_t \mathbb{E}[\text{err}_t] - \alpha \right| = 0.$$

□

A.5 Additional figures

We begin by giving three figures showing the results for Section 4 in the case where we use a variable value for η , given by $\eta = \eta_t = \sqrt{\frac{\log(500 \cdot k) + 2}{\sum_{s=t-500}^{t-1} \mathbb{E}[\ell(\beta_s, \alpha_s)^2]}}$. We see that the results are nearly exactly identical to those obtained with the fixed heuristic choice of η .

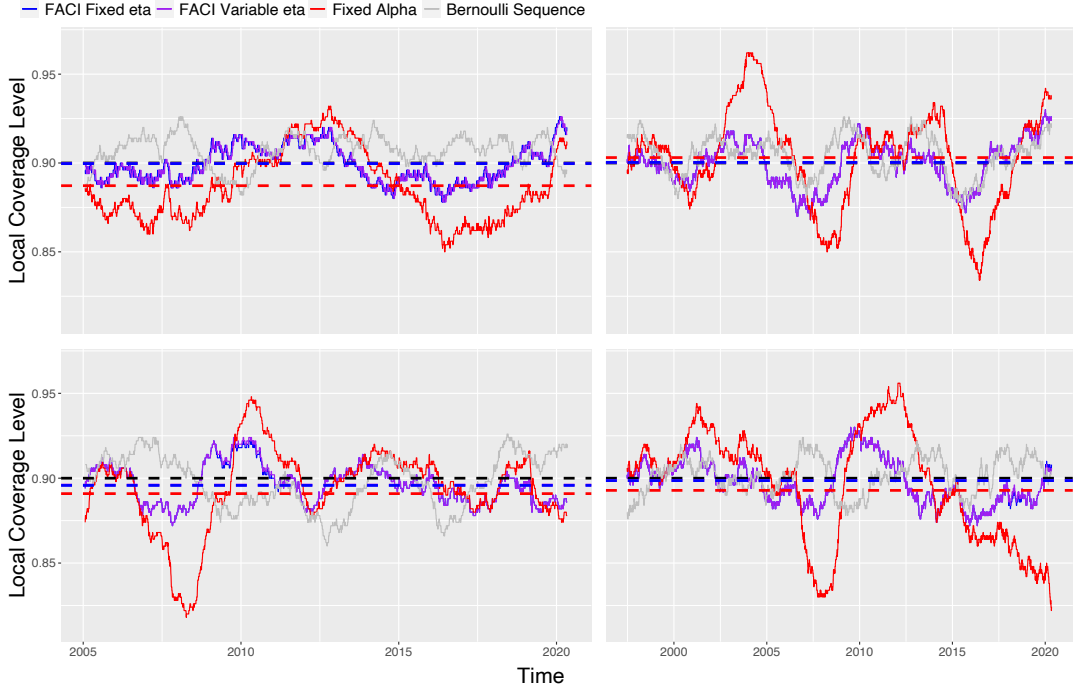


Figure A.1: Estimation of stock market volatility using conformity score $S_t(v) = |v - (\hat{\sigma}_t^t)^2|/(\hat{\sigma}_t^t)^2$ and $\eta_t = \sqrt{\frac{\log(500-k)+2}{\sum_{s=t-500}^{t-1} \mathbb{E}[\ell(\beta_t, \alpha_t)^2]}}$. Solid lines show the local coverage level for $\bar{\alpha}_t$ with variable (purple) and fixed (blue) eta, a naive baseline that holds $\alpha_t = \alpha$ fixed (red), and an i.i.d. Bernoulli sequence (gray). Dashed lines indicate the global coverage frequency over all time steps for the same methods. The black dashed lines indicates the target level of $1 - \alpha = 0.9$.

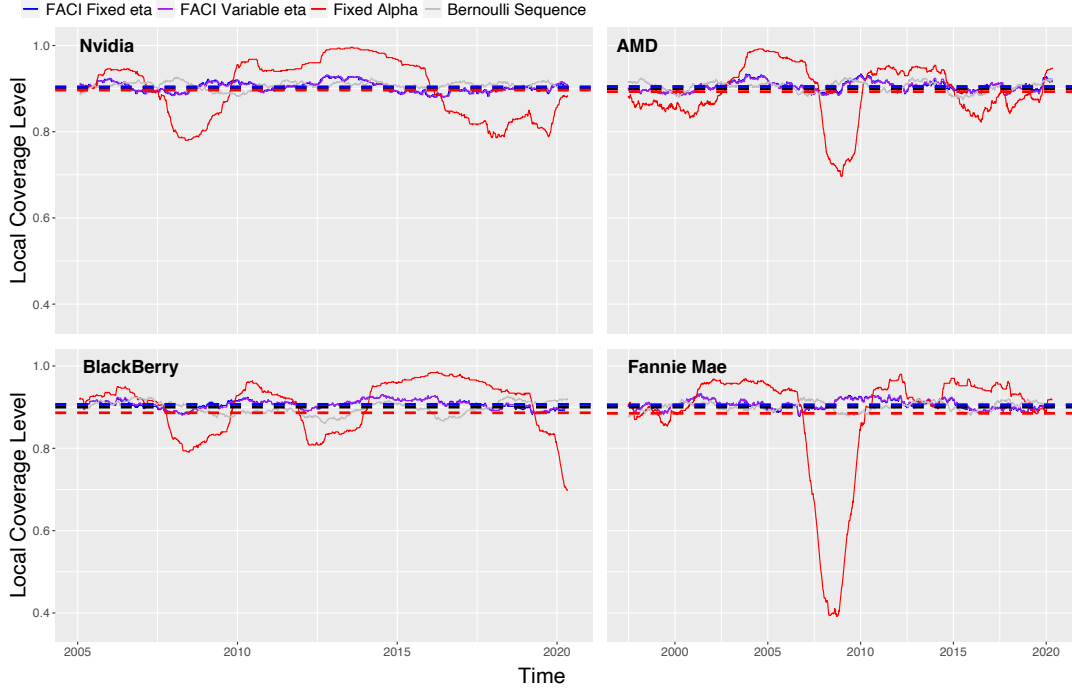


Figure A.2: Estimation of stock market volatility using conformity score $S_t(v) = |v - (\hat{\sigma}_t^2)|$ and $\eta_t = \sqrt{\frac{\log(500-k)+2}{\sum_{s=t-500}^{t-1} \mathbb{E}[\ell(\beta_t, \alpha_t)^2]}}$. Solid lines show the local coverage level for $\bar{\alpha}_t$ with variable (purple) and fixed (blue) eta, a naive baseline that holds $\alpha_t = \alpha$ fixed (red), and an i.i.d. Bernoulli sequence (gray). Dashed lines indicate the global coverage frequency over all time steps for the same methods. The black dashed lines indicates the target level of $1 - \alpha = 0.9$.

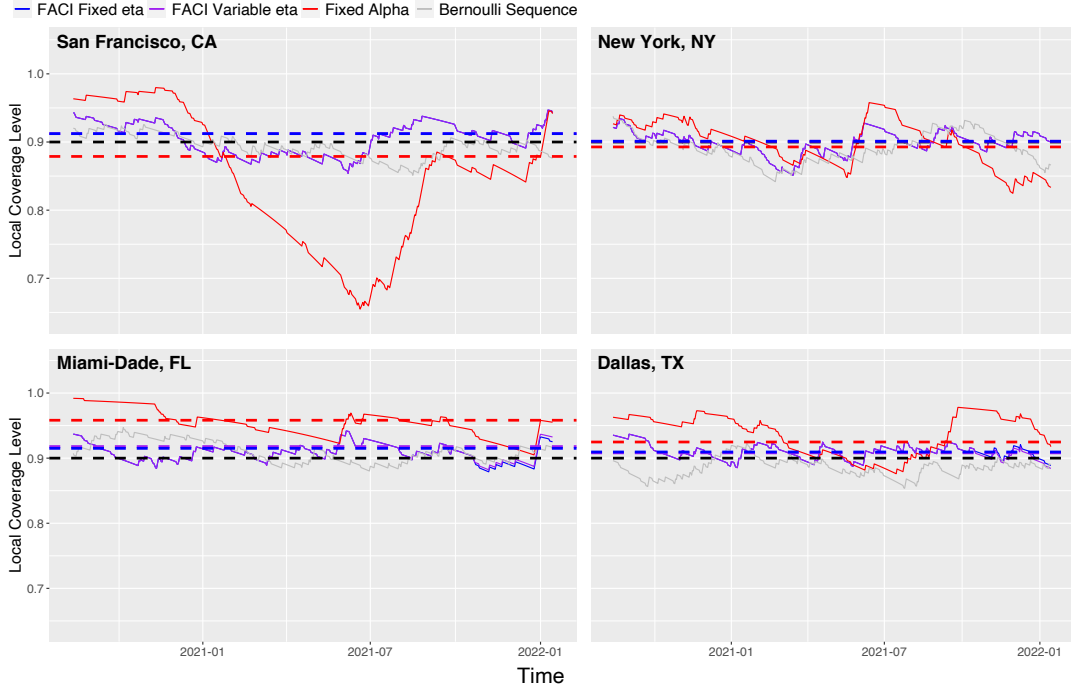


Figure A.3: Coverage results for the prediction of county-level COVID-19 case counts with $\eta_t = \sqrt{\frac{\log(500 \cdot k) + 2}{\sum_{s=t-500}^{t-1} \mathbb{E}[\ell(\beta_t, \alpha_t)^2]}}$. Solid lines show the local coverage level for $\bar{\alpha}_t$ with variable (purple) and fixed (blue) eta, a naive baseline that holds $\alpha_t = \alpha$ fixed (red), and an i.i.d. Bernoulli sequence (gray). Dashed lines indicate the global coverage frequency over all time steps for the same methods. The black dashed lines indicates the target level of $1 - \alpha = 0.9$.

Our next figure shows the empirical conditional coverage (4.2) for the estimation of stock market volatility with the unnormalized conformity score. As for the normalized conformity score we observe conditional coverages close to the target level across all values of $\bar{\alpha}_t$.

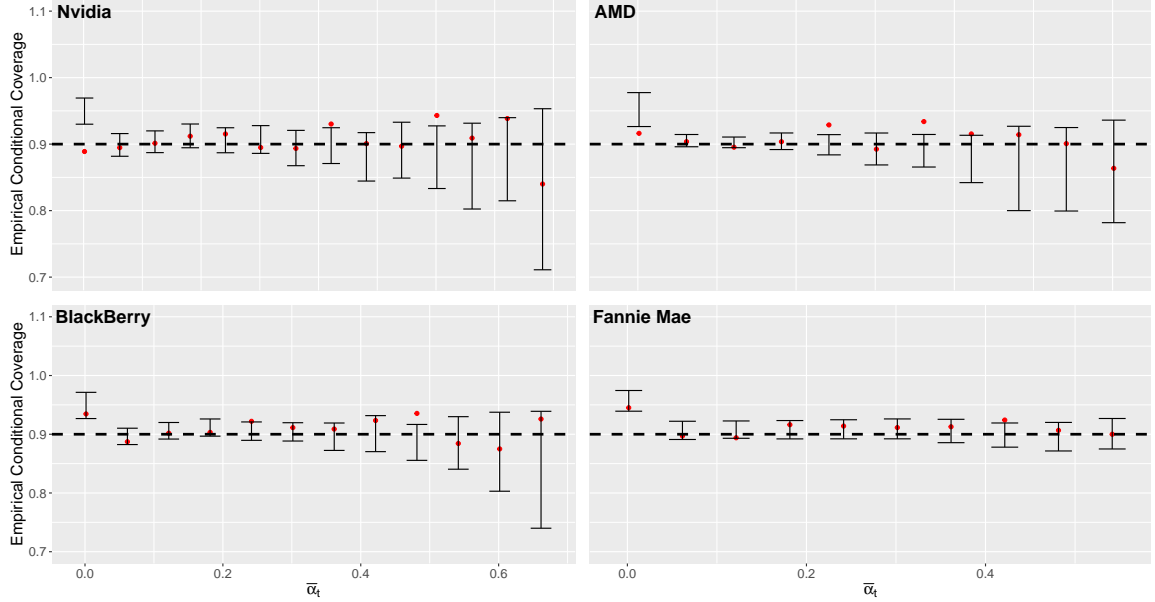


Figure A.4: Empirical conditional coverage of $\bar{\alpha}_t$ for the estimation of stock market volatility with conformity score $S_t(v) = |v - (\hat{\sigma}_t^t)^2|$. Red points show the empirical conditional coverage given $\bar{\alpha}_t \in B_i$ with error bars indicating the corresponding 0.05 and 0.95 quantiles across 100 block bootstrap resamples of the data $\{(X_i, Y_i)\}$ with block-size set to 100. Black dashed lines shows the target level of $1 - \alpha = 0.9$.

Finally, Figures A.5 and A.6 show the stock prices and the COVID-19 case counts for the datasets considered in Section 4.

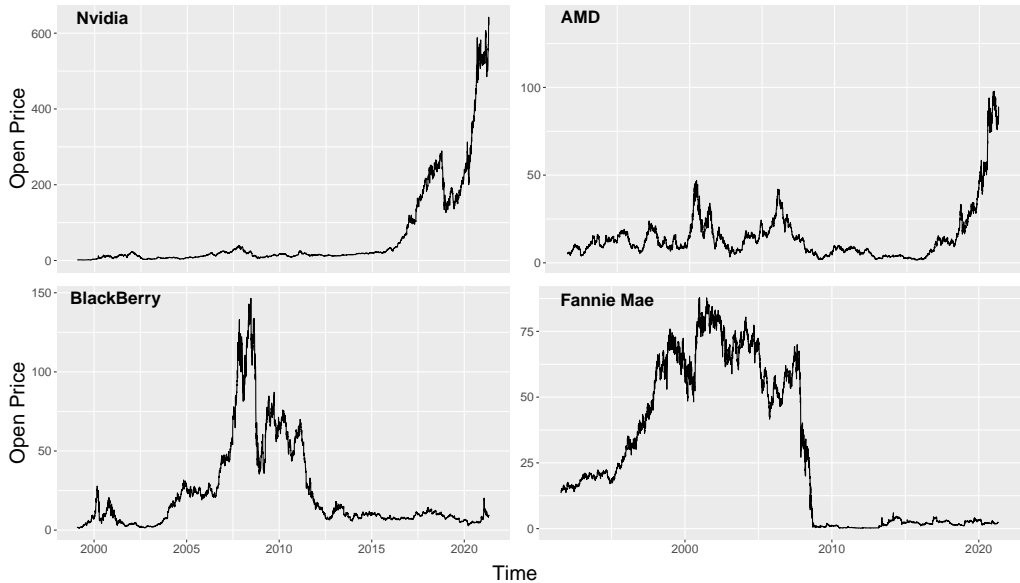


Figure A.5: Daily open prices for the four stocks considered in Section 4.1.

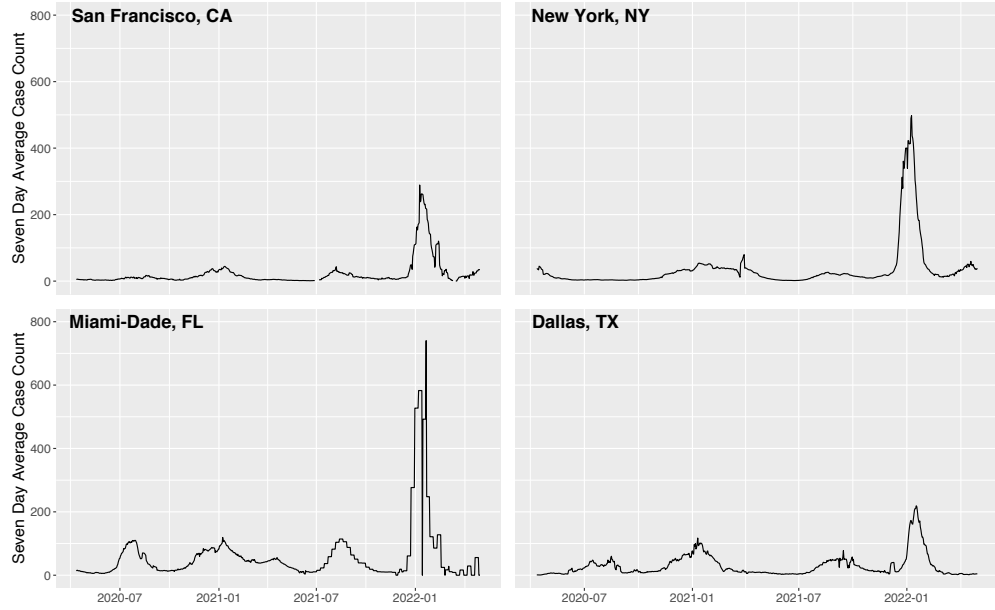


Figure A.6: Moving seven day averages of the number of new confirmed COVID-19 cases per 100,000 people in the four counties considered in Section 4.3.